Accepted Manuscript

Electric field gradients and bipolar electrochemistry effects on neural growth: A finite element study on immersed electroactive conducting electrode materials

Llibertat Abad, Ann M. Rajnicek, N. Casañ-Pastor

PII: S0013-4686(19)31082-5

DOI: https://doi.org/10.1016/j.electacta.2019.05.149

Reference: EA 34290

To appear in: *Electrochimica Acta*

Received Date: 22 January 2019

Revised Date: 17 May 2019

Accepted Date: 28 May 2019

Please cite this article as: L. Abad, A.M. Rajnicek, N. Casañ-Pastor, Electric field gradients and bipolar electrochemistry effects on neural growth: A finite element study on immersed electroactive conducting electrode materials, *Electrochimica Acta* (2019), doi: https://doi.org/10.1016/j.electacta.2019.05.149.

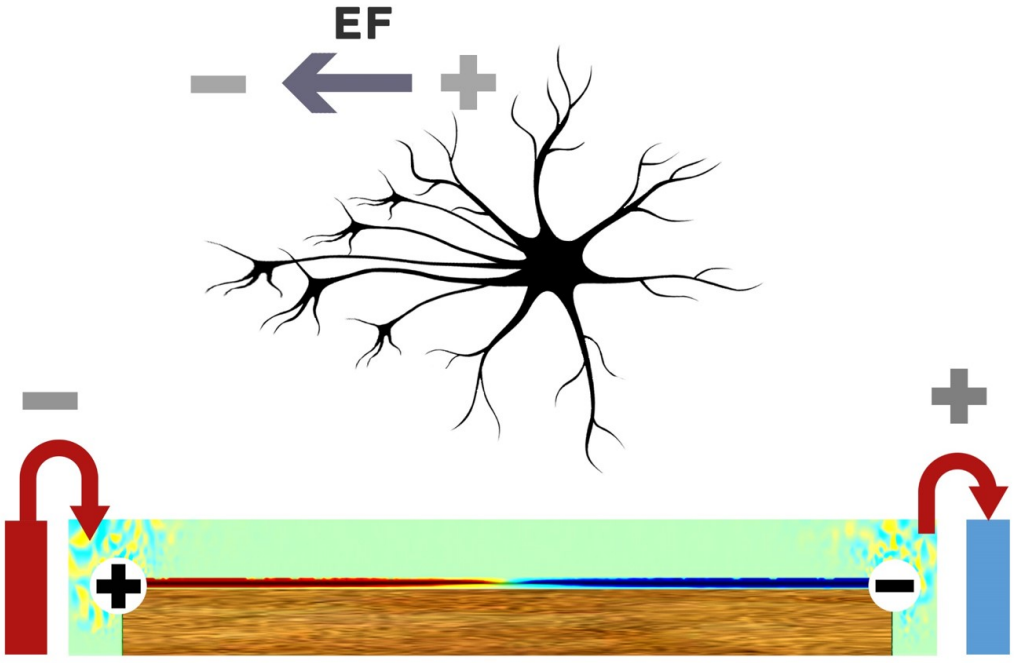

Electric Field Gradients and Bipolar Electrochemistry effects on Neural Growth: A finite element study on immersed electroactive conducting electrode materials.

Llibertat Abad[1], Ann M. Rajnicek[2], N. Casañ-Pastor[3]*

[1] Institut de Microelectrònica de Barcelona, Centro Nacional de Microelectrónica (IMB-CNM-CSIC). Campus de la UAB, E-08193, Bellaterra (Barcelona), Spain.; [2]University of Aberdeen, School of Medicine, Medical Sciences and Nutrition, Institute of Medical Sciences, Aberdeen, AB25 2ZD, UK; [3] Institut de Ciencia de Materials de Barcelona, CSIC, Campus UAB. 08193 Bellaterra, Barcelona, Spain. Email: nieves@icmab.es

Abstract

Implantable electrodes act with direct electrical contact although recent work has shown that electrostimulation is also possible through non-contact wireless settings, through the generation of dipoles at the borders of the material by bipolar electrochemistry. The experimental observations with neural cell cultures demonstrate a clear difference between insulator and conducting materials, but also between conducting and mixed conducting intercalation materials used as substrates of neural growth. Known bipolar electrochemistry effects may explain voltage profiles induced on conducting materials. Finite element studies shown here with the same configuration that the experimental processes described, evidence voltage profiles in qualitative agreement with known bipolar effects, although with a clear difference between intercalation materials and metals. Calculations also show a clear mapping of charge gradients at the material surface influencing growing neurons cells. While insulating materials only distort the electric field space distribution, the dipole generated at the borders of an implanted conducting material, inverted with respect to the insulating case, extends along the material interface, being relevant that is much smoother in intercalation materials. Mapping of the gradients as the distance is increased from the conducting material is also discussed. These observations may explain the differences in neural cell growth observed for various substrate materials.

Keywords: electric gradients, neural electrodes, charge asymmetry,

finite elements, electroactive materials, implants

1. Introduction

Effects of electric fields in alternating (AC) and direct (DC) voltages have been studied in vivo and in vitro with electrodes in direct connection with the tissues and/ or cells implanted [1-18]. DC fields are known to modify neural development in vitro for neurons adhered to insulating materials and also on conducting materials [15-18]. Repair has also been induced using large capacity electrodes [19]. Although ionic gradients present in the electrolytes are proposed to be responsible of neural growth [18], the influence of the specific material on which cells grow is significant but unclear. Roughness, chemical aspects and charge capacity values in intercalation electrodes that allow safer charge injection in the biological system, are known to be determinant.

Recently, unconnected conducting materials used as substrates for neural growth have been shown to elicit different neural responses, in presence of an external driving field, thanks to the induced dipole in the material borders [20]. The induced dipole at the material borders, of opposite sign than the driving field, may reach potentials sufficient to split water in H_2 and O_2 with the corresponding increase and decrease of pH at the induced cathode and anode respectively. But within the safe aqueous potential window other effects may be reached. The reactions induced by creation of such a dipole are often called bipolar electrochemistry and occur at the boundaries of the conducting material immersed in the electrolyte following fundamental physics laws [21-23]. It was suggested in the 60´s with fluidized beds [24] but developed more recently in the field of materials and nanotechnology. Bipolar electrochemistry has been nicely described previously and multiple applications of interest in materials and nanotechnology shown [22,23,25] like asymmetric deposition, gradient material formation, and also resulting physical properties gradients like conductivity, electrochromism or even motility depending on the redox intercalation properties, redox processes or size of the material as few examples. [21,25] Physico-chemical calculations and quantifications has also been developed [26,27] including equivalent circuits usually assuming that the bipolar materials does not affect the ionic electrolyte conditions, in cases of purely electronic conducting materials.

In terms of cell growth and response on conducting electrostimulation electrodes, the specific ohmic drops through the electrolyte may be affected, and ionic gradients and conductivity of the material are suspected to be crucial in the final induced potentials of the dipole and therefore in cells responses, resulting in a complex system of interactions between ionic gradients induced by the external field and the dipole. Geometry of the electric field applied is of course also decisive.

In particular, when the material is not only conducting electronically, but also undergoes redox intercalation reactions, as in the mixed conducting intercalation materials, bipolar electrochemistry effects induce asymmetric intercalation and therefore changes in conductivity, color and other physical properties of the material may occur in an asymmetrical way, as shown before [22,28]. From the biological point of view, such chemical asymmetry and the resulting asymmetry in properties, may introduce additional effects to those of the electrolyte gradient -derived effects, because of the material-cells interaction. This in turn may cause specific cell responses. Recent experimental observations indeed show that neural cells grown on IrOx or PEDOT behave differently in the absence and in the presence of an external driving field. IrOx favors the speed of neural growth while PEDOT-PSS based materials favor turning towards the driving cathode [20]. The chemical characteristics of each material, or the gradients induced in them by bipolar effects seemed significant. Electrodeposited IrO_x is an

amorphous oxohydroxide of approximate formula $K_{1.7}IrO_{0.8}(OH)_{2.2}.1.5H_2O$ and the best substrate found for neural cell growth in mammalian cases. Studies have demonstrated its ability to intercalate and deintercalate the existing structural K^+ ion and also Na^+, H^+ and OH^- ions from solution [10] On the other hand all conducting polymers, specifically PEDOT-X, (with X being the anionic counterion used, ex. PSS polysterene sulfonate) also undergo cation and anion intercalation reactions under oxidation and reduction that induce conductivity, color and volume changes, although large X anions prevent anion mobility. For the largest volume changes, bionic elements may be designed, while highly biocompatible polymers are reached when the anion part of the polymer is an aminoacid such as lysine [13]. In the case of IrOx, hybrids with nanocarbons have been created with largely enhanced charge capacities [29-31], which in turn has shown the possibility of short term repair in some models of neural cell wounds [19].

Although in both cases electrostimulation with these electrodes connected to the power source show specific responses [19], in bipolar electrochemistry conditions with no direct contact and the material is immersed in the cell culture medium, it has been surprising to discover that neural cells also develop and grow on some materials, and, depending on the material, with enhanced speed or changing their growth direction [20]. In particular, intercalation mixed-valence materials favor a completely different behavior in cells. The fundamental physics behind the effects on cells are not well known, although the most reasonable assumption is the modification of the charge gradient within the electrolyte and /or the substrate material. Such a qualitative explanation has been offered in a previous work in terms of bipolar electrochemistry [20], but additional effort is needed to understand the environment in which cells are growing, to study possible differences of bipolar effects for either metallic conducting or mixed conducting materials, mapping voltage and charge profiles that could eventually explain such behavior.

This work represents a first approach, considering the known bipolar electrochemistry effects, of evaluating the voltage profiles along with the ionic gradients within the electrolyte and materials surfaces on which cells adhere, and the nearby environment. Although deep studies have been carried out in bipolar electrochemistry work in terms of voltage profiles and applications [21-28,32,33], and mapping of isovoltage curves had been shown before in two-dimensional microchannels [33], voltage and charge gradient mapping in cell culture usual geometries could potentially offer explanation for specific differences among electroactive materials influencing cell growth in different ways. A finite element model (FEM) could approach such mapping in a reasonable fashion. Thus, insulating and conducting materials are compared (ex. glass vs gold immersed materials) when immersed in an electrolyte, in a first step, and the expected bipolar effects observed. In a second stage, intercalation materials allowing ion diffusion within the material structure are considered. Graphite has been chosen as the prototype of redox intercalation, both cationic and ionic, because it was the first known material to undergo those processes [34] and diffusion parameters are known for it. In all cases, a charge gradient profile is studied according to a space distribution calculated by finite element high resolution contributions, in order to establish the basic physical parameters behind. The magnitudes of potential gradients induced in the material, the electrolyte and the interaction among them, are evaluated using finite element calculations using COMSOL Multiphysics software [35]. Being aware of the influence of electrodes and electric field geometries, the calculations shown here use the same field geometry used in previous work

with application of electric fields to cell cultures, where neural cell growth and direction was evaluated [20]. Calculated charge profiles evidence a smoothing of bipolar electrochemistry effects in the materials that allow intercalation, while also showing that the whole surface of the material substrate of neural growth is affected for all conducting cases. Also, a clear influence of bipolar effects related to the conducting material can be seen at the electrolyte that surrounds it, in profiles that are microns away from the materials surface. Lower peak voltages are found always in intercalation materials and therefore a full difference with respect to standard bipolar electrochemistry expected effects on pure electronic conducting materials.

Direct bipolar electrochemistry effects on neural cells themselves cannot be neglected by any means, since cells may be considered discrete particles [23,24], and including them in the calculation is part of a further study. However, since experimental work kept that variable constant, the first step in our opinion deals with the materials response in bipolar conditions.

2. Experimental and Calculations

The finite element model used is based on COMSOL software (COMSOL Multiphysics 5.4 using the Electrostatic module, and stationary solutions) and is used considering boundary conditions that resemble an electrochemical cell geometry with the dimensions and geometry of the experimental set ups and the different driving electric fields used in ref [20]. The complexity included mimics exactly the experimental set up cell culture. External driving electrodes are considered to be metallic silver, to prevent additional polarization effects (conductivity 61.6x 10^6 $S.m^{-1}$ and density 10500 $kg.m^{-3}$). The cell geometry chosen also mimics experimental geometry, dimensions and arrangement as in reference [20] where observations of dipolar effects have been reported, instead of usual capillary systems considered in bipolar electrochemistry [21-28,32,33]. The set up considered is schematized in Figure 1a: the immersed material, 30 mm in length is placed in the center of the medium electrolyte. Distances are given with respect to the center of that material piece. The possible gradient of ions in some materials (graphite cases) is also schematized in Figure 1b.

Several cases are considered in parallel as schemes of the experiments previously reported, taking an electrolyte defined with the same ionic strength that the one used experimentally in ref [20], namely NaCl (58 x 10^{-3}M), KCl (0.07 M), $Ca(NO_3)_2$ (0.44 x 10^{-3}M) and $MgSO_4$ 1.3 M, namely adding up to 0.06 M^+ global cationic concentration. The electrolyte is considered present in salt bridges and through membranes. Electric conductivity is considered to be 10 S/m (and relative permittivity 5) within the driving electrodes media, and 1 S/m (relative permittivity 40) in the environment of cell culture, to emulate experimental cell culture media. Usual electrolytes in the neural system have large ionic concentrations depending on the species but in general there is a low resistivity, 0.5 Ω.m, at the exoplasma (1-2 Ω.m within the neurons) [36,37].

Insulating cases are considered as immersed material as well as conducting metals with similar relative dimensions. Borosilicate glass and pure gold are taken as respective examples in both cases, with conductivities 45.6x10^{-6} S/m and 45.6x10^6 S/m respectively (library data in [26]). Being a material that allows intercalation and therefore become mixed conductor and because

diffusion parameters are known, graphite is taken as example of intercalation conducting material, using various maximum doping degrees (0.33 and 0.5 charge carriers/C atom). Conductivity of 100 S/m is taken in both cases and also for both 1.43x 10^{-13} diffusion coefficients. This last case is the most complex and approximate since many variables from materials such as IrOx, PEDOT-PSS and related phases in a certain doped state are not known, but the approximation is considered valid as a first approach to quantify the induced field magnitude, distribution and the ionic gradients created. Additional parameters for each material are shown in Supplementary material.

Figure1

The materials under study are considered immersed into an electrolyte of concentration also similar to the experimental set ups in ref [20]. External Ag electrodes are imposing an electric field, and the effects at the interface electrolyte/material are evaluated, depending on its electric properties and redox intercalation possibilities. The distance between external driving electrodes is kept equal to the experiments described (30 cm apart) [20]. And also the distance between material and external electrodes (15 cm between center of sample and external electrodes, and 3 cm total length of immersed material).

The voltage and charge solution created on the *Comsol Multiphysics* software v.5.4 [35], for each external driving voltage, corresponds to the stationary field that will drive ionic movement and electrochemical processes, fulfilling ohmic drop considerations, Ficks law of diffusion and Butler-Volmer equations [35,38] to account for overpotentials at the immersed electrodes. Overvoltage's at the material borders have been calculated by subtracting the electrolyte voltage drop at each position without subtractions from possible water splitting reactions at the highest potentials.

The triangular finite element mesh (shown in Figure 1) chosen for calculations has been optimized after asymptotic convergence of the solution for each specific applied voltage, using noise and pole symmetry as well as stable induced dipole as criteria. The space that surrounds the immersed material has been allowed for smaller element size, from a maximum of 0.001 m to a minimum of 1x10^{-9} m. Convergence is achieved at larger resolution values (120 vs 100) for the high voltage case, and for Graphite intercalation material. Oscillations in those last steps of convergence are considered to be the implicit error of the model.

Voltages between driving electrodes chosen for calculations, although arbitrary, are in the same range than those used in previous experimental work. In this analysis we chose 1V difference and, to simulate our previous experimental work in which live neurons were used, we also used voltages per unit length of 50 mV/mm and 150 mV/mm. These correspond here to 15 V and 50 V over the 30 cm distance between external electrodes in the model. The 150 mV/mm situation is a potential where H_2 and O_2 production and corresponding pH changes were observed previously in the electrolyte, while 15 V is not [20]. pH changes used as reference were evaluated using phenol red (yellow when acidic, bright pink when alkaline).

Charge and voltage profiles are calculated in the three-dimensional system but extracted for simplicity from a one-dimensional horizontal line that includes the material surface, where cells will eventually be adhered. Additional multiprofile analyses are included up to 10 µm height from the immersed material, for evaluation of effects at the neural cell dimensions. The origin of the main axis in the dimension x is taken in the zero potential zone in the center of the conducting material, as usual [21] even though any possible voltage drop anisotropy may shift that position. Final global overvoltages in the material are calculated subtracting the

electrolyte voltage drop at each position. Although the existence of solvent reactions has been accounted before by subtracting a constant voltage in the cell [33], this work manipulates only the raw data with respect to the electrolyte voltage drop, to observe the influence of ions diffusion/intercalation in graphite on bipolar voltages.

A multiple profile voltage analysis is also done at distances up to 10 microns from the material surface

3. Results and Discussion

Calculations shown in this work take into account imposed voltage ranges where key points are observed in experimental observations, specifically pH changes and metal stripping (Ti adhesion layer used on Au electrodeposited, and gets oxidized at some potentials) observed at the poles of the conductive materials. [20]. See Figure 2. No pH changes are observed for 50 mV/mm but are clearly seen for 150 mV/mm, with simultaneous gas evolution, H_2 (g) and O_2 (g) respectively at the induced cathode (in front of the driving anode), and induced anode (in front of the driving cathode). The 100 mV/mm case is similar to the 150 mV/mm case in smaller extent. Therefore, those extreme two values, 50 and 150 mV/mm, are taken as reference points for calculations, as 15V and 50V in this work.

Figure 2.

Large element size and low resolution calculations tend to yield asymmetric results among poles and result in significant noise in the case of larger voltages and when ion diffusion is considered in the material (graphite). Even with the same absolute resulting voltage among poles, convergence reduces noise and improves symmetry among them. It is reasonable to assume that this noise derives from the triangular element shape, and therefore element size and curvature are allowed to be modified as explained in the experimental part. It is also relevant to mention that the intrinsic voltage drop derived from electrolyte resistance may confer a different relative error in each pole of the immersed material (see Table 1). A final convergence error is found for all calculated voltages in the order of 10% in terms of symmetry of voltage at both poles. Further asymmetry related to intercalation behavior is expected and predicted by the finite element model , and is discussed below.

Figures 3, 4 show the stationary spatial solution for the voltage (Fig 3a and 3b) and charge (Figure 3c) gradients observed upon application of external fields of different magnitude. In the case of immersed glass, the insulating character of the material induces a small distortion in voltage change, while the ohmic drop from the electrolyte reduces the actual voltage between the immersed glass borders. Accordingly, the change in charge distribution in the environment of the glass borders results evident but the charge gradient at the glass border near the driving cathode remains negative, and remains positive in front of the external anode. For immersed glass, the magnitude of the charge gradient is directly proportional to the imposed voltage, about 3 to 11 x 10^{-4} C/m^3 per volt imposed.

If gold is immersed however, an inverted potential dipole is created between the poles the conducting piece, as expected in bipolar electrochemistry [21-28], and an induced voltage between poles much larger in absolute value that the one for glass. (See Figure 3 and Table 1 for quantified Voltage (V) and Charge (Q) gradient values at the surface of the material for

each applied voltage). Further detail for immersed gold subtracting the electrolyte voltage drop, shows no field in the central part of the metal as expected, (see Figure 4b) and a positive deviation over the electrolyte straight line (voltage drop) in front of the driving negative electrode, simultaneous with a negative voltage deviation in front of the positive driving electrode. (Figure 4). Again, as indicated in bipolar electrochemistry works, this results in an induced anode and an induced cathode respectively at the borders of the immersed gold piece. With respect to the glass example, as mentioned above, this represents an inversion of voltage profiles at the borders of the material as described also qualitatively in ref [20]. To this point, the finite element model is showing what bipolar electrochemistry predicts. (See further discussion below for charge profiles)

Figure 3. a) b) c)

Table 1

Figure 4a,b.

Figure 5.

Figure 6.

Considering immersed graphite examples in Figure 4, a similar behavior is also observed, but with smaller dipole voltage in cases of 1 and 15V applied. The voltage profiles at the borders of the material are smoother in graphite than in gold.

An axial multiprofile analysis up to 10 µm in height, the size of neural nuclei, shows a smooth lowering of about 30% of the dipole induced in the Au case, and still the same sign of the dipole.

In terms of electric field, the differences in dipole profile are even more evident, (see Figure 5, the derivative of the potential along the main axis of the electrochemical cell in the region of the material immersed). The peaks observed correspond to the largest magnitudes of the field, at the material borders and coincide with maxima in the charge gradient. Gold has the sharpest field change right at the border of the material, but also a considerable distortion in the electrolyte near each border, approximately 0.01 m in size. Graphite on the other hand show the same type of gradient but without the sharp peaks, with the maximum dipole is 75% that of Au, and without reaching a zero value within the material, as expected for a semiconductor. The shape of the field profile, must derive from the diffusion and intercalation of ions within graphite. In graphite cases, the voltage multiprofile, also shows a continuous decrease as the position gets far from also shows a lower dipole starting point (75% in voltage vs that of Au for the 15V external field) at the surface of the material, but the dipole is still present at the 10 µm distance. (Figure 6). Neurons growing on such material therefore will see a dipole 75% in strength, but also with smoother spatial gradient.

Simultaneously, it is clear that a larger portion of the material surface is involved in the intercalation material graphite as compared to Au. Ion diffusion in the material is again considered as responsible for such difference, and also the main difference that is expected to

be affecting cell behavior on those materials. It is intuitive to expect that smooth voltage or charge profiles will affect neural cells in different fashion than sharp and abrupt spatial changes. This part of the modelling could be in essence describing experimental observations in ref [20], where cell grown on Au behaved quite differently than in intercalation materials.

Quantification of the dipoles induced in each material and for each potential applied externally and maximum charge gradients are shown in Table 1. As observed, the induced dipoles in graphite are smaller than in gold for the two lower external potentials applied, 1 V and 15 V, beyond the estimated error of the method. At 50 V external voltage applied, the dipoles are slightly larger in graphite, but within the estimated 10% error, See Table 1 and Figure 6b. At the potential range in which intercalation and ion diffusion within the graphite structure may occur, (15 V here) a smaller dipole is indeed expected in graphite as compared to gold, since ion intercalation would lower the charge accumulation at the borders of the material where dipole is created. Graphite 0.5 , is also expected to have a lower dipole voltage than Graphite 0.33, since the extent of ion diffusion is larger in absolute value. Calculations show that this is true at 15 V, in agreement with electrochemical intercalations.

A multiprofile analysis is shown in Figure 6b for the case of 15 V external applied voltage, which corresponds to the optimal conditions for neural cell culture in [20] and no water splitting present. Profiles show that the bipolar effect expands beyond the size of a neuron body, 10 µm, although with dipoles that slowly decrease as the distance to the conducting material is increased. In the case of intercalation materials, the same behavior is also seen with a lower potential at the starting point. Arrows in Figure 6b represent the largest deviation from the electrolyte ohmic drop, and correspond to about half of the potential than at the surface of the material.

Furthermore, the dependence of the dipole voltage with the external voltage applied is not linear in any of the cases, but it is quite different for gold and graphite (See Figure 6a). Although non-linearity in induced voltage vs applied voltage has been discussed before for metals by Duval [28], the reasons for that are not known. In the case of semiconductors like graphite, and additional consideration must be taken into account, in our opinion, derived from the thermal activation threshold that may be overcome at some voltage. That could indeed modify the conductivity of graphite, and has been considered specifically in the calculation.

As discussed above, an error in dipole voltages is estimated in terms of asymmetry even after convergence, derived from the finite element configuration. But also significant is the asymmetry observed and expected for graphite intercalation materials. M^+ ions would diffuse within the material at the induced cathode, and may diffuse out at the induced anode. That possible ionic diffusion within the material in the cases where redox intercalation is possible (graphite in this work) would create ionic gradients that will result in a real asymmetry at the poles. Indeed, the larger voltage asymmetries between poles are observed in those cases.

Also significant is the spatial shift that this effect induces of the zone with potential near zero. (see Figure and 5, x axis). In the case of Graphite 0.5 is shifted with respect to Graphite 0.33 and this with respect to gold. This spatial shift, clearly related with the asymmetric intercalation processes may have a direct effect on electrode positioning in biological systems, as described before [20]

Charge gradients profile right at the material surface and borders reflect the corresponding voltage and intercalation effects. Deep spikes at the material borders are observed in all cases (Figure 3c), with magnitudes shown in Table 1. Convergence results in symmetric spikes at induced cathode and anode, and absolute charge gradients that increase with the applied voltage (Figure 3c). All conducting examples have charge gradients of opposite signs than those observed for an insulating material, as expected, but also larger in size. An interesting value derives if charge is considered per volt applied, since it defines a capacity behavior for the material surface immersed. Au has larger gradient values per volt than Graphite 0.33, but Graphite 0.5 results very similar to Au, and in all cases, within the estimated 10% error of the method. The global capacity of charge gradients created versus the voltage applied remains similar for all materials tested and therefore the conductivity properties seem to be the essential part. Voltage profiles however had been shown above to differentiate better the profile at the material surface.

A zoom at the material corner at the highest voltages shows an alternating of negative and positive layers with triangular crown shape in the pole regions with stronger voltage peaks (see Supplementary material Figure S1). Such shape derives clearly from the finite element shape. However, lowering element size up to four orders of magnitude beyond convergence retains that alternating of positive and negative charges showing that the charge wave is a real effect, although no its shape. This calculated charge gradients, in form of ripples, add to the known features. Thus, in front of the induced anodic pole, negative charges accumulate and a second layer of an opposing positive zone of smaller magnitude is also created behind, something not predicted in previous bipolar electrochemistry works [21-28]. (See Figures 3-6). This suggests the presence of low intensity waves that try to compensate the direct charge accumulation resulting from the induced pole. A double layer type of behavior and wave formation would also make physical sense. Thus, the complexity of ionic distribution, even in this one dimensional case, suggests complex interactions and dynamics. If neurons or other cells, which have inherent electrical properties and significant membrane voltages, were to be included in the system, it is reasonable to suggest that additional electrical effects and reciprocal interactions between cells and materials would exist, possibly varying regionally. Indeed, different cell behaviors have been found before for different materials such as iridium oxide, PEDOT, polypyrrole and graphene, as well as hybrids of them, and such interaction needs to be accounted for. [20,39]

As expected from the potentials observed at the borders of the conducting materials and predicted before in bipolar electrochemistry publications [21-28,32,33] the charge gradients calculated have also the opposite sign than those observed in the insulator glass case, (See Figure 3 and Table 1). For higher fields, such as those used in previous experiments (between 50 mV/mm and 150 mV/mm, here corresponding to 15 V and 50 V, for the 30 cm distance between external electrodes assumed here), charge gradients of ± 30 x10 $^{-4}$ C/m^3 per volt applied, and opposite to the electrolyte gradient (or the insulator material case). Therefore, in the surface of the material and direct media in touch with it, the field and charge have been inverted, with the absolute magnitude of the charge gradient two times larger than for an insulator.

The observed charge gradient at the materials poles corresponds to changes of 2 $x10^{-11}$ moles of ions/liter as compared to the 0.06 moles/liter electrolyte volumic concentration, or as usually stated [36,37], 1.2 $x10^{20}$ univalent ions/liter. However, the gradient is local and may be significant because is concentrated in the 10 µm height regime, the size of neurons bodies, which are cultivated in a media in the range of 4 x 10^{15} ions/m^2 [36,37]. This comparison emphasizes that the electric field gradients calculated for the experimental conditions, have magnitudes that may well affect neuron development and behavior, and yield additional use to mapping through FEM.

A significant point of the calculated charge gradient is the large extension of the material surface affected as for voltage gradient both in the 50 mV/mm and the 150 mV/mm cases. (See Figure 3c) (It is worth remarking here that 150 mV/mm applied voltage induces water splitting with corresponding pH changes near the immersed conducting material). So, the FEM model renders an induced dipole with a defined "front" depending on the geometry of the conducting piece, the conductivity and the electrolyte concentration. Such front has been also observed experimentally; if Au is deposited on Ti, the oxidation of Ti strips off the Au with a similar "front" shape [20]. As the calculation has been implemented on a material with sharp edges, equal to the experimental piece, the significance of abrupt potentials at those points may be considered. On the other hand, all effects observed derive from the boundary between a conducting material and a non-conducting one. Further developments with more complex structures and other geometries are planned in future work.

An additional effect is seen when observing the dependence of induced voltage versus applied voltage for all materials. Although quasilinear, the gold case shows a saturation, and larger imposed voltages do not result in proportional effects. However, Graphite does not show the effect in the same extent, and the induced voltage is closer to linearity. As the main difference between materials relates to the mixed conduction in Graphite, again, it is possible that the intercalation /diffusion of ions in the material is at the root of such behavior. Even more, being graphite the best known example of intercalation [34], and since doping is variable, differences are seen for two extents of doping, Graphite 0.33 and Graphite 0.5, with equal diffusion and conductivity assumed in the finite element model [35]. (See supplementary material for parameters used at finite elements calculations library). The first observation has been that intercalation defines ion diffusion in the material and therefore the voltage profile within the material is not flat and the derivative is smoother, as seen in Figure 4-6. Correspondingly, the positive and negative deviations of potential at the induced anode and cathodes are not symmetric in spatial distribution and shape. Such effects are larger for larger intercalation possible, Graphite 0.5. As far as we know the mapping of these charge and voltage effects have never been calculated neither observed in bipolar electrochemistry studies, and offer additional insight on the environment that cells seed at the material surface are truly sensing.

Also, the existence of the dipole on the conducting material, about -9V for 50 V imposed for example) is correlated with a lower ohmic drop at the electrolyte nearby (-12 V at glass border and -9 at conducting material, see Figure 4a). That permits a significant conclusion; since the presence of a conducting material lowers the global ohmic resistance of the cell at that profile

height, this may be important for the design of clinical implants, that would allow also a smaller imposed field to reach the same induced dipole.

A significant point is how that voltage profiles change smoothly as the distance from the material surface increases, since neural cells contain bodies about 10 microns in diameter, and respond to ionic gradients. The multiprofile analysis indeed explains that all parts of the cell are affected by the induced dipole in conducting Au, and in a different way in intercalation graphite materials with smooth dipoles.

Relation of graphite with IrOx and PEDOT

It is worth discussing here the similarities between graphite taken as a model in this work and other intercalation materials tested experimentally. IrOx is an oxohydroxide with mixed valence state (Ir^{+3}- Ir^{+4}) and has "room" for both oxidation and reduction to full Ir^{+4} or full Ir^{+3}, without complete loss of conductivity. During that process, cations present in the media may intercalate in the induced cathode through reduction, and anions in the induced anode through oxidation. Alternatively, anions may be released from the cathode and cations from the anode, since IrOx is an oxohydroxide with H^+ and K^+ and OH^- in its structure [10].

PEDOT-PSS on the other hand, is in the oxidized form when prepared, and it is susceptible to cation redox intercalation at the induced cathode but its PSS component is not able to leave the structure, hindering anion intercalation at the anode. It is also possible to reach "overoxidation" of the polymer main structure at the induced anode (external driving cathode), which would become insulating [13-14]. The immediate consequence is that the conducting region of the original material is decreased and therefore the dipole is present in a smaller space. Thus, upon the same driving external field, the dipole induced may be different for IrOx or PEDOT-PSS because of the front advance related to changes in conductivity.

The type of intercalation present is also different for each material due mostly to structural effects, and each material may accommodate different types of ions differently. Thus, besides conductivity and carrier concentration, the ionic identity in each extreme of the material may also be different. This aspect has not been considered in our calculations but the profiles indicate the stationary state that could drive such intercalations. Despite that, the gradients calculated for graphite as an example of an intercalation process indicate shapes and forms of the electric field that could be important, with no significant differences for the two extents of intercalation.

Since finite elements software assumes the same diffusion coefficient for both graphite types, only conductivity and the fact that ion diffusion does exist within the material can account for differences with respect to gold. Gold has been taken as an example where only electronic conductivity would affect the results. Our model confirms this because an induced dipole of opposite sign is created as for Au, but graphite shows a different dipole magnitude and a softened voltage and charge gradients at the borders that modify the geometry of the dipole and possibly the whole surface potential and ionic gradient to which cells will be sensitive. So,

there is a clear difference between just electronic conducting materials and mixed ionic-electronic conducting materials. Previous work [19,20,29-31] has shown that to be true experimentally, since intercalation in mixed conducting materials involves lower impedance and larger charge capacities [19, 29-31], which results finally in short term repair and in clear differences in behavior for neural cells grown on them.

Experimental observations of Xenopus neuronal cells show neuron turning towards an externally imposed cathode [16]. When a material is immersed in the electrolyte the effect of field distortions or induced dipoles at the borders of the conducting materials, modifies neural behavior as reported. This work shows how a new ionic gradient is created in the case of conducting materials, and how intercalation mixed conducting materials show voltage and charge profiles that are clearly different from metallic cases, in complete agreement with experimental observations. It is relevant to mention an additional fact. Ionic gradients created at the poles, and surface, of the materials to which cells would adhere increase as the external field increases, in directions that follow the external field, if the material is insulator, or that oppose the external field imposed, for conducting and mixed conducting materials. Despite that opposed polarity, neurons continue growing towards the external cathode [20]. However, compared with an insulating substrate, the speed of nerve process outgrowth in metallic substrates such as Au or Pt was slower, but it was faster on intercalation materials like PEDOT or IrOx based materials, specially IrOx [Figure 6 in ref [20]]. It would seem, therefore, that the dipole effect on Au decreases neuronal outgrowth speed. Significantly, this does not apply to an intercalation material where speed was increased, and where this work shows that a smooth dipole is created. Graphite, taken in this paper as an example of intercalation material, would represent specially IrOx because both are able to undergo intercalation of cations and anions at the negative and the positive poles respectively (and the opposite if field is reversed). In those cases, the voltage profile is not flat, because of ionic diffusion within the immersed material allows that smoothing effect and the charge gradient profile consequently is different. That could explain the slower neural growth on gold electrodes as compared to glass, and to “softer” profile- intercalation materials.

In addition, mixed conducting electrodes have ionic gradients within the structure that could reinforce such growth speed, as observed in IrOx that contains K+ and may intercalate and deintercalate Na^+, K^+ , H^+ and OH^-, or direction effect as observed in PEDOT-PSS. In particular, the induced cathode part of the material undergoes M^+ intercalation, something possible in graphite, IrOx or PEDOT-PSS [10,13,14]. X^- intercalation would occur at the induced anode, to counteract oxidation redox changes, and it may occur in IrOx and graphite but however is not expected to be possible in PEDOT-PSS, due to the large doping state present and the large size of PSS that involves not additional X^- intercalation possible [14 and ref therein] and no possible deintercalation of PSS. The simulations performed in this work with asymmetries between poles and softened spatial profiles in voltage and charge that would be expected from different intercalation processes in the anode and cathode, could be the origin of the observed differences between IrOx and PEDOT-PSS.

4.Conclussions

This work simulates the voltage, charge and field gradients created when a conducting material is immersed in an electrolyte under an external applied field and directly affects the

study of interactions of cells with implanted materials. While the voltage profile does not get actually inverted, an overpotential is created at each pole with respect to the electrolyte at each point of the spatial profile, making possible the existence of a locally inverted electrochemical cell, called usually bipolar electrochemistry. The stationary solution obtained in this study explains the opposed polarity in charge distribution on immersed conducting electrodes without direct contact to the circuit but it goes beyond the classical studies in bipolar electrochemistry. It also shows a significant mapping of the gradient along the material surface, existing also at heights above the material larger than the size of the neuron body, and a dipole front that is not simple and may extend to the whole material surface exposed to cells, especially on intercalation materials, as well as a soften pole voltage and charge distribution. Furthermore, the dependence of voltage induced between poles with the external field in mixed valence conductors is different from electronic conductors and larger dipoles may be created for the same external field. That could significantly explain the behavior of cells grown on gold or any conducting material, versus those grown on glass, and also the different behavior of cells grown on IrOx or PEDOT vs those grown on gold.

Experiments at high fields have shown that such front propagates as the substrate under Au gets oxidized, and also as the PEDOT induced anode gets overoxidized [20]. But even without accounting for irreversible oxidation, the charge gradient calculated here evidences the complexity of the profile even in one dimension, due to the interaction of the material with the ionic electrolyte and the existence of the inverted charge distribution.

In addition to cell growth rate favored by the intercalation materials, that could be taken as a measure of a driving force, the magnitude of the turning towards the external cathode is also significant in the experimental observations, being especially large for PEDOT-PSS materials. The calculations shown here cannot show evidence in that sense, but could suggest that the ionic gradient observed for PEDOT will differ from that created in IrOx, as the former paragraph discusses. An increased cationic concentration in a particular material, or the ionic balance between induced cathode and anode sides, could define an increased turning angle of cell dendrites.

Our work shows that better understanding of the complex and dynamic electrochemical properties of conductive materials in bipolar situations would allow to tune them to particular active medical implants and applications. For example, as indwelling electrodes designed to stimulate or impede axon growth, or even to guide axons to appropriate targets. This modelled mapping may help in the experimental search of specific cationic gradients for each of these applications in vitro and in vivo.

The implications of these electric gradients on electrode implants results in effects beyond standard connected systems. Even cells could induce dipolar effects on the implanted material, and in that case, undergo an effect from the dipole induced, opening the possibility of wireless electric stimulation paths. Further theoretical development involving cells is a complex task but worth the effort.

Acknowledgments: This work was funded by the European Commission FP6 NEST Program (Contract 028473), RTI2018-097753, MAT2011-24363 and MAT2015-65192-R from the Spanish Science Ministry, La Marató de TV3 Foundation (Identification Number 110131), and Severo Ochoa Programme for Centres of Excellence in R&D (SEV-2015-0496). LI. Abad thanks MINECO

for a Ramón y Cajal Contract (RYC-2013-12640). The authors also thank A. Beardo (NanoTransport group from UAB) for useful discussions.

References

[1] S. Shapiro, R. B. Borgens, R. Pascuzzi, K. Roos, M. Groff, S. Purvines, R. B. Rodgers, S. Hagy, P. Nelson, J Neurosurg. Spine 2 (2005) 3-10.

[2] S. Harkema, Y. Gerasimenko, J. Hodes, J. Burdick, C. Angeli, Y. Chen, C. Ferreira, A. Willhite, E. Rejc, R. G. Grossman, V. R. Edgerton, The Lancet 377 (2011) 1938-1947.

[3] C. A. Angeli, V. R. Edgerton, Y. P. Gerasimenko, S. J. Harkema, Brain 137 (2014) 1394-1409.

[4] A. A Fomani, R. R. Mansour, C. M. Florez-Quenguan P. L. Carlen, J. Microelectromech. Systems 20 (2011) 1109-1118.

[5] S. B. Brummer, M. J. Turner, Bioelectrochem. Bioenerg. 2 (1975) 13-25.

[6] D. R. Merrill, M. Bikson, J. G. R. Jefferys, J. Neurosci. Methods 141 (2005) 171-198.

[7] S. F. Cogan, Annu. Rev. Biomed. Eng. 10 (2008) 275-309.

[8] S. J. Wilks, S. M. Richardson-Burns, J. L. Hendricks, D. C. Martin, K. J. Otto, Front. Neuroeng. 2 (2009) art. 7.

[9] S. Venkatraman, J. Hendricks, Z. A. King, A. J. Sereno, S. Richardson-Burns, D. Martin, J. M. Carmena, Neural Systems and Rehabilitation Engineering, IEEE Transactions 19 (2011) 307-316.

[10] A. M. Cruz, L. Abad, N. M. Carretero, F. J. Moral-Vico, P. Lozano, G. Subias, V. Padial, M. Carballo, J. E. Collazos-Castro, N. Casañ-Pastor, J. Phys. Chem. C 116 (2012) 5155-5168.

[11] T. Boretius, M. Schuettler, T Steiglitz, Artificial Organs 35 (2011) 245-248.

[12] N. K. Guimard, N. Gomez, C. E. Schmidt, Prog. Polymer Sci. 32 (2007) 876-921.

[13] J. Moral-Vico, N. M. Carretero, E. Pérez, C. Suñol, M. Lichtenstein, N. Casañ-Pastor, Electrochim. Acta 111 (2013) 250-260.

[14] Toktam Nezakati, Amelia Seifalian, Aaron Tan, and Alexander M. Seifalian, Chem. Rev., 118 (2018) 6766–6843.

[15] A. M. Rajnicek, K. R. Robinson, C. D. McCaig, Dev. Biol. 203 (1998) 412-423.

[16] A. M. Rajnicek, L. Foubister, C. D. McCaig, J. Cell Sci. 119 (2006) 1723-1735.

[17] R. W. Davenport, C. D. McCaig, J. Neurobiol. 24 (1993) 89-100.

[18] A. M. Rajnicek, N.A.R. Gow, C. D. McCaig, Exper. Physiol. 77 (1992) 229-232.

[19] M. P. Lichtenstein, E. Pérez, L. Ballesteros, C. Suñol, N. Casañ-Pastor, Appl. Mater. Today 6 (2017) 29-43.

[20] A.M. Rajnicek, Z. Zhao, J. Moral-Vico, A.M. Cruz, C.D. McCaig, N. Casañ-Pastor, Adv. Healthcare Mat. 7 (2018) 1800473

[21] S. E. Fosdick, K. N. Knust, K. Scida, R. M. Crooks, Angew. Chem. Int. Ed. 52 (2013) 10438-10456.

[22] L. Koefoed, S. U. Pedersen, K. Daasbjerg, Current Opinion in Electrochemistry 2 (2017), 13–17

[23] G. Loget, D. Zigah, L. Bouffier, N. Sojic, A. Kuhn, Acc. Chem Res. 46 (2013) 2513–2523.

[24] M. Fleischmann, J. Ghoroghchian, D. Rolison, S. Pons, J. Phys. Chem. 90 (1986), 6392 – 6400

[25] G. Loget, J. Roche, E. Gianessi, L. Bouffier, A. Kuhn, J. Am. Chem. Soc. 134 (2012), 20033−20036.

[26] F. Mavré, K.-F. Chow, E. Sheridan, B.-Y. Chang, J. A. Crooks, R. M. Crooks, Anal. Chem.81 (2009), 6218 – 6225.

[27] J. F. L. Duval, G. K. Huijs, W. F. Threels, J. Lyklema, H. P. van Leeuwen, J. Colloid Interface Sci. 260 (2003), 95 – 106.

[28] J. F. L. Duval, J. Buffle, H. P. van Leeuwen, J. Phys. Chem. B 110 (2006), 6081 – 6094

[29] N. M. Carretero, M P. Lichtenstein, E. Perez, L. Cabana, C. Suñol, N. Casañ-Pastor, Acta Biomaterialia 10 (2014) 4548-4558.

[30] N.M. Carretero, M. P. Lichtenstein, E. Pérez, S. Sandoval, G. Tobias, C. Suñol, N. Casan-Pastor, Electrochimica Acta 157 (2015) 369-377.

[31] E. Pérez, M. P. Lichtenstein, C. Suñol, N. Casan-Pastor, Materials Science & Engineering C 55 (2015) 218-226.

[32] J. Duval, J. M. Kleijn, H. P. van Leeuwen, J. Electroanal. Chem. 505 (2001), 1 – 11

[33] S. E. Fosdick, J. A. Crooks, B. Chang, R. M. Crooks, J. Am. Chem. Soc. 132 (2010), 9226–9227

[34] M. S. Dresselhaus, G. Dresselhaus, Advances in Physics 51 (2002) 1-186.

[35] COMSOL Multiphysics® Software, version 5.4. (www.comsol.com). COMSOL AB, Stockholm, Sweden.

[36] R.K. Robbie, B.J. Roth “Intermediate physics for Medicine and Biology” Springer Sci., New York (2007).

[37] G.L. Pollack, D.R. Stump, “Electromagnetism”, Addison-Wesley, San Francisco (2002).

[38] P.T. Kissinger in “Laboratory techniques in Electroanalytical Chemistry”, P.T. Kissinger, W.R. Heineman eds., Marcel Dekker, Inc., New York (1984).

[39] N. P. Pampaloni, M. Lottner, M. Giugliano, A. Matruglio, F. D’Amico, M. Prato, J.A. Garrido, L. Ballerini, D. Scaini, Nature Nanotecnology 13 (2018) 755–764

FIGURE CAPTIONS

Figure1. A) Complete set up used in calculations with 30 cm distance between external electrodes and salt bridges for ionic contact, with zone where material is immersed expanded below. Finite element mesh described with increased resolution in the material environment. Material (blue) immersed in an electrolyte in presence of an external driving electric field. The - electrode, which is the driving cathode, is at the left, and the + electrode, which is the driving anode, is at the right). The profile in the expanded image corresponds to expected electrolyte voltage drop. B) Scheme of ionic gradients where the material may undergo redox intercalation, shown as M+ intercalation at the negative induced pole.

Figure 2. pH changes observed for various Au thin layers (Au 15 nm on Ti 5 nm coated glass, as described in ref. [14]) immersed electrodes, in presence of external driving fields of 50, 100 and 150 mV/mm (driving cathode on left, driving anode on the right). The pole in front of the driving anode undergoes H_2 and OH^- production with corresponding raise in pH, while the pole in front of the driving cathode undergoes O_2 and H^+ production.

Figure 3. Spatial Voltage (a) and Charge gradients (b) for 1, 15 and 50V (3.33, 50 and 150 mV/mm, in profile and colored mapping

Figure 4. a) Voltage Profile at the material surface height for 1, 15 and 50 V and each material. b) Spatial distribution of overpotentials for immersed materials with respect to the electrolyte ohmic drop at the material surface height.

Figure 5. Representative Spatial profile of Electric field distribution for 15 V applied voltage (from derivative of V vs Distance)

Figure 6. a) Induced voltage in the material borders vs applied potential, b) Voltage Multiprofile from the material surface to 10 µm altitude above, at 15 V applied , for Au and Graphite 0.33. The representative case corresponds to experimental settings in which neural cells were cultured and without water splitting reactions.

TABLE CAPTION

Table 1. Calculated voltages at the poles of the materials and Induced dipole between the borders of the immersed conducting material using the electrolyte ohmic drop as reference and the Maximum Charge gradient observed in each profile.

Supplementary material

Scheme S1. Parameters of the various materials in the calculation from COMSOL Library

Figure S1. Real Local charge waves at material border showing shapes derived from the element triangular shape

External driving Voltage (V)	**1**	**15**	**50**
Voltages between poles for each material (V)			
Glass left	-0,0258	-0,38	-1,58
Glass right	0,04	0,47	1,36
Total voltage between poles	**0,066**	**0,85**	**2,94**
Au left	0,183	2,88	6,81
Au right	-0,18	-2,56	-5,22
Absolute Dipole for Au	**-0,36**	**-5,44**	**-12,03**
Graphite 0.33 left +	0,175	2,19	7,23
Graphite 0.33 right –	-0,116	-1,98	-6,55
Absolute Dipole Graphite 0.33	**-0,291**	**-4,17**	**-13,78**
Graphite 0.5 left +	0,159	1,92	8,36
Graphite 0.5 right –	-0,135	-2,19	-4,2
Absolute dipole Graphite 0.5	**-0,294**	**-4,11**	**-12,56**
Maximum Charge gradients per unit voltage Q/V at the material surface profile $(C/m^3/V) \times 10^{-4}$			
Glass	6	38	34
Au	-60	-60	-69
Graphite 0.33	--54	-54	-62
Graphite 0.5	-69	-70	-62

Table 1

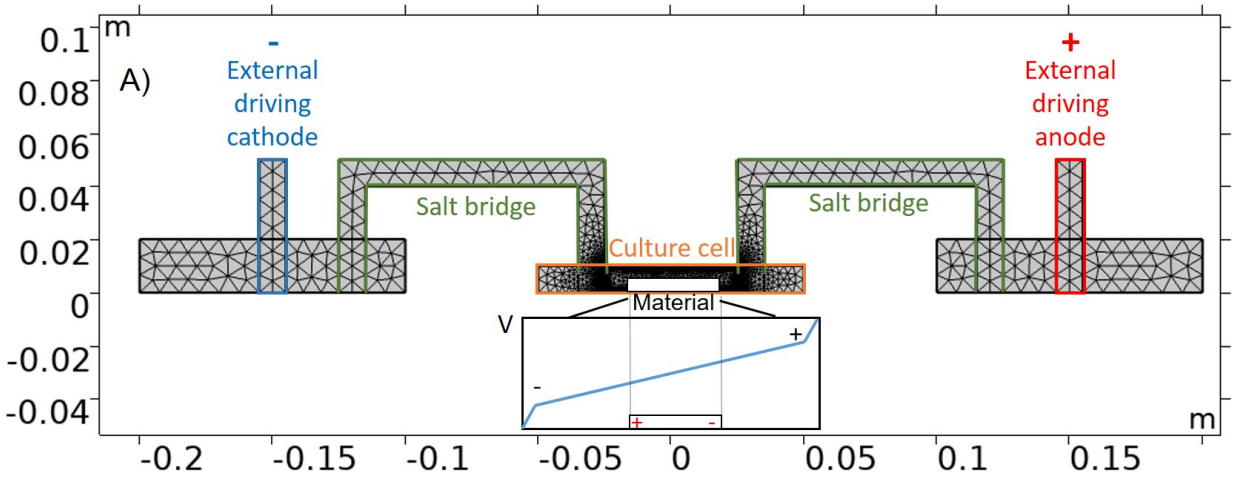

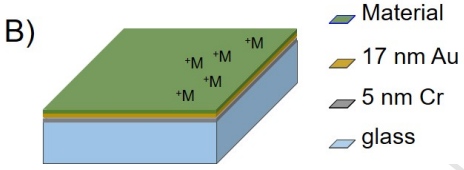

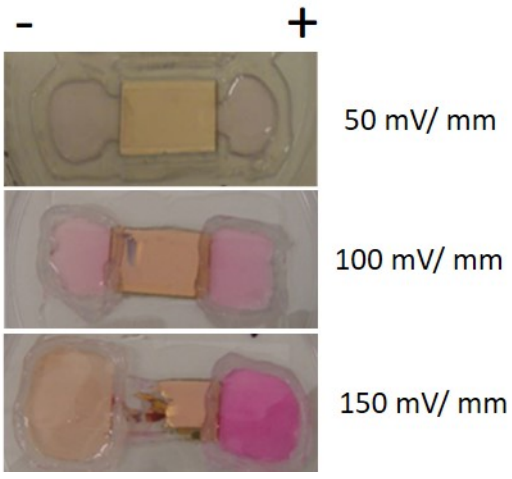

Figure 3a

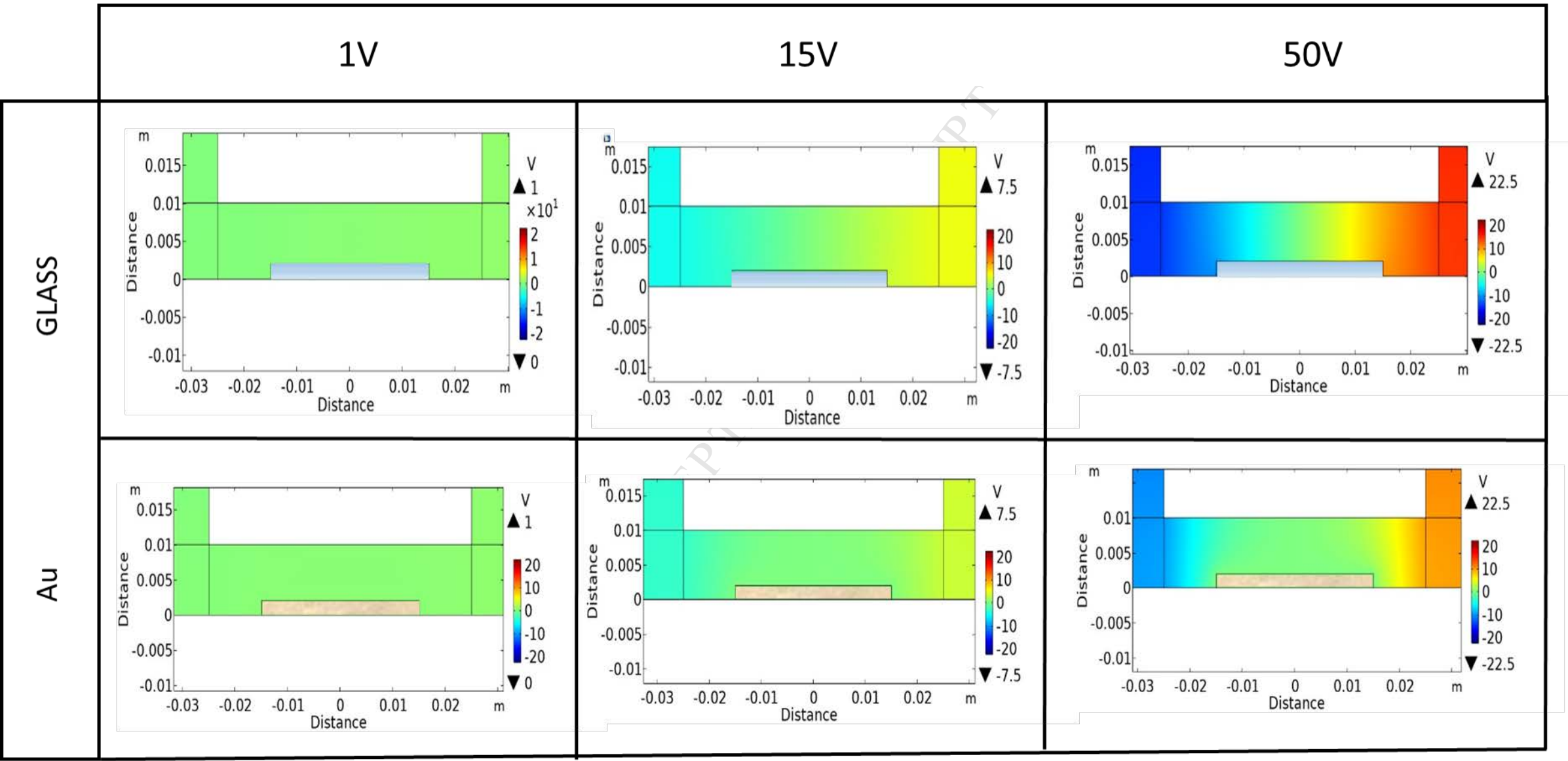

Figure 3b

	1V	15V	50V
Graphite 0,33	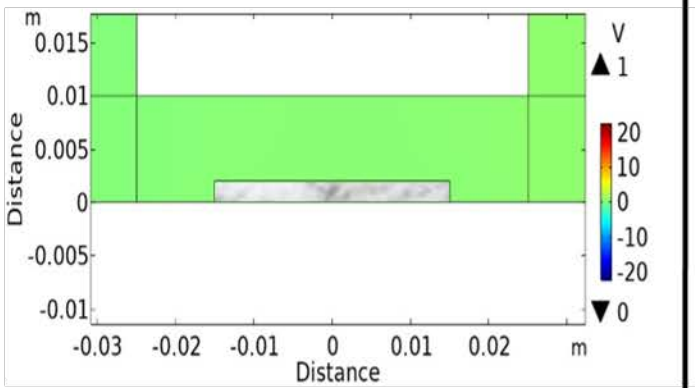	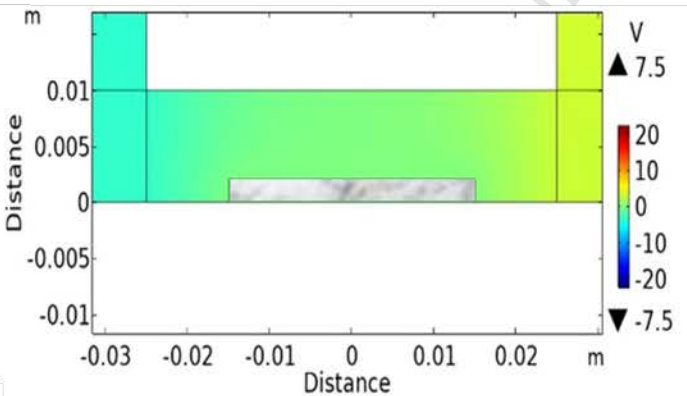	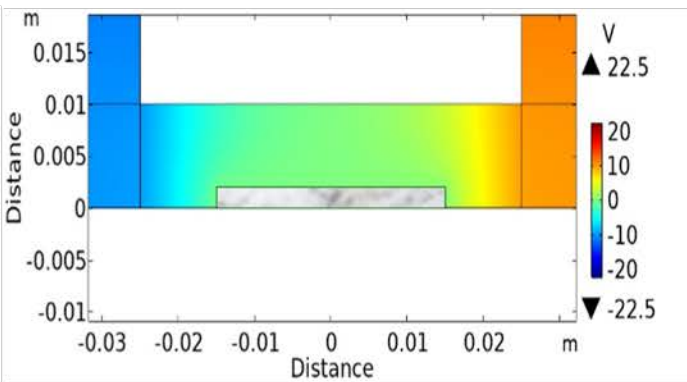
Graphite 0,5	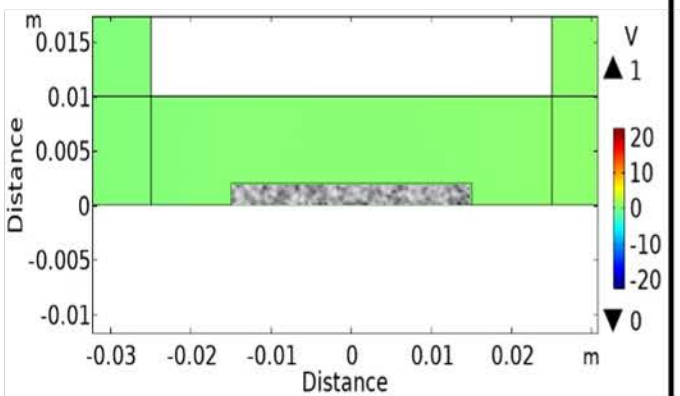	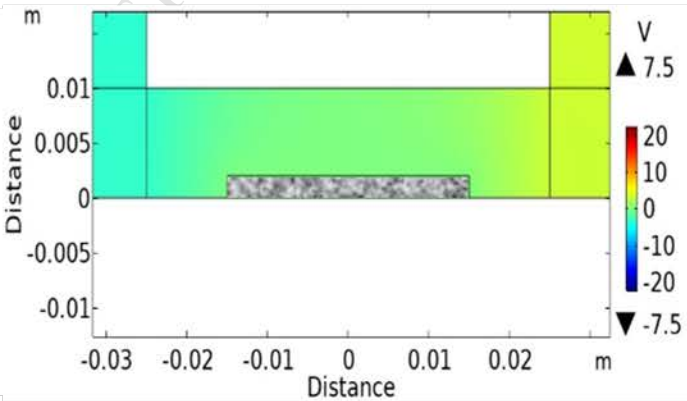	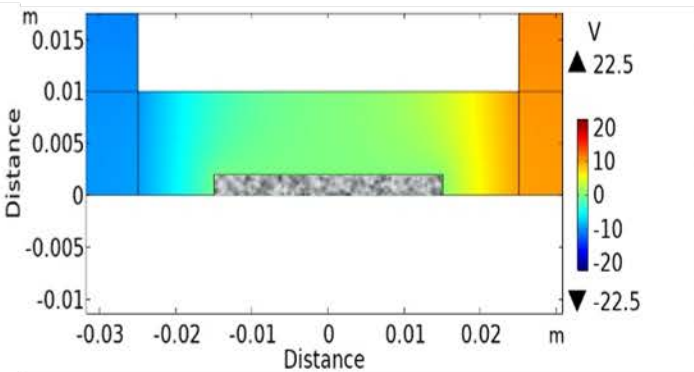

Figura 3c

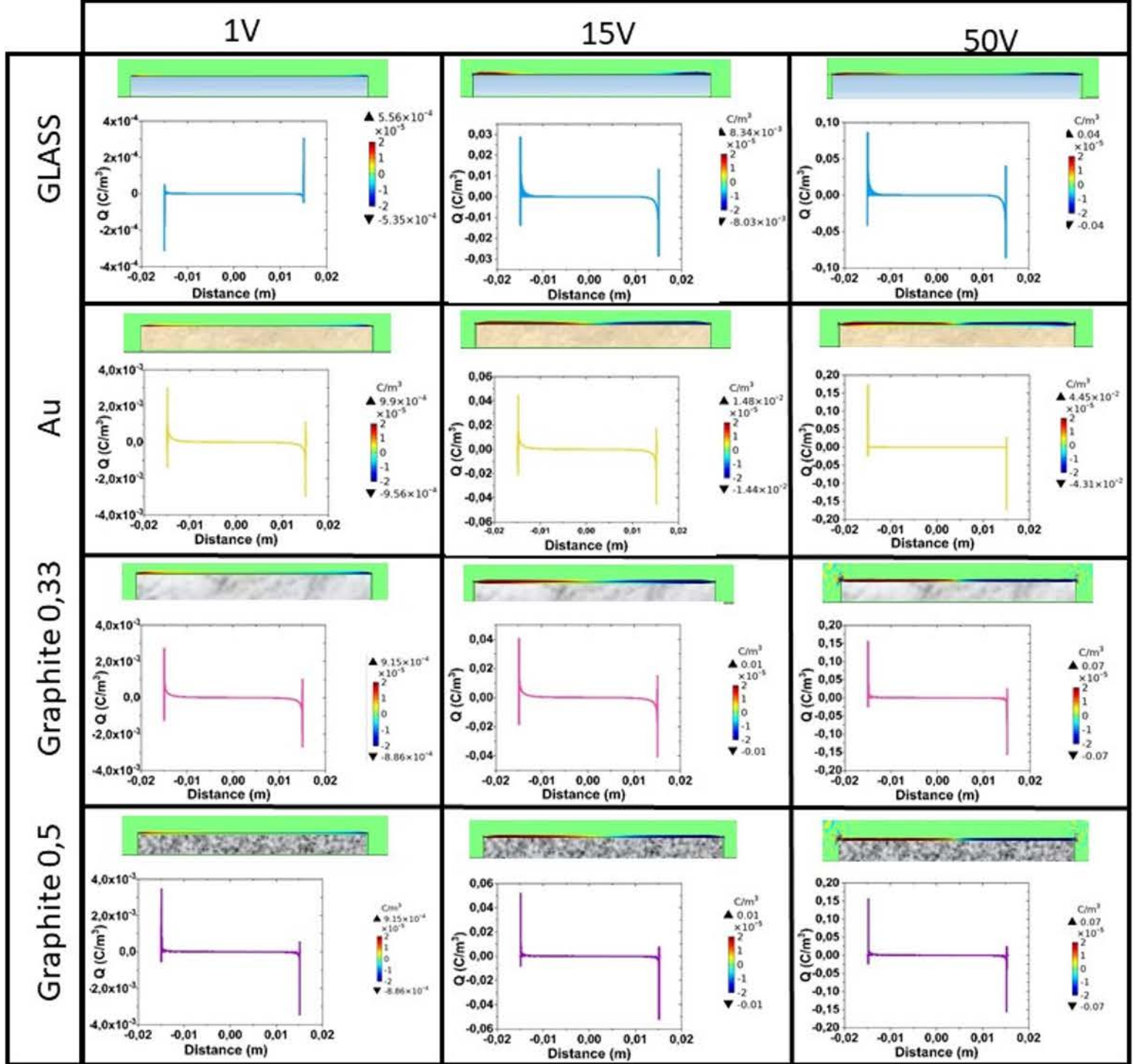
1V
15V
50V
GLASS
Au
Graphite 0,33
Graphite 0,5
Q (C/m³)
Distance (m)
C/m³

Figure 4

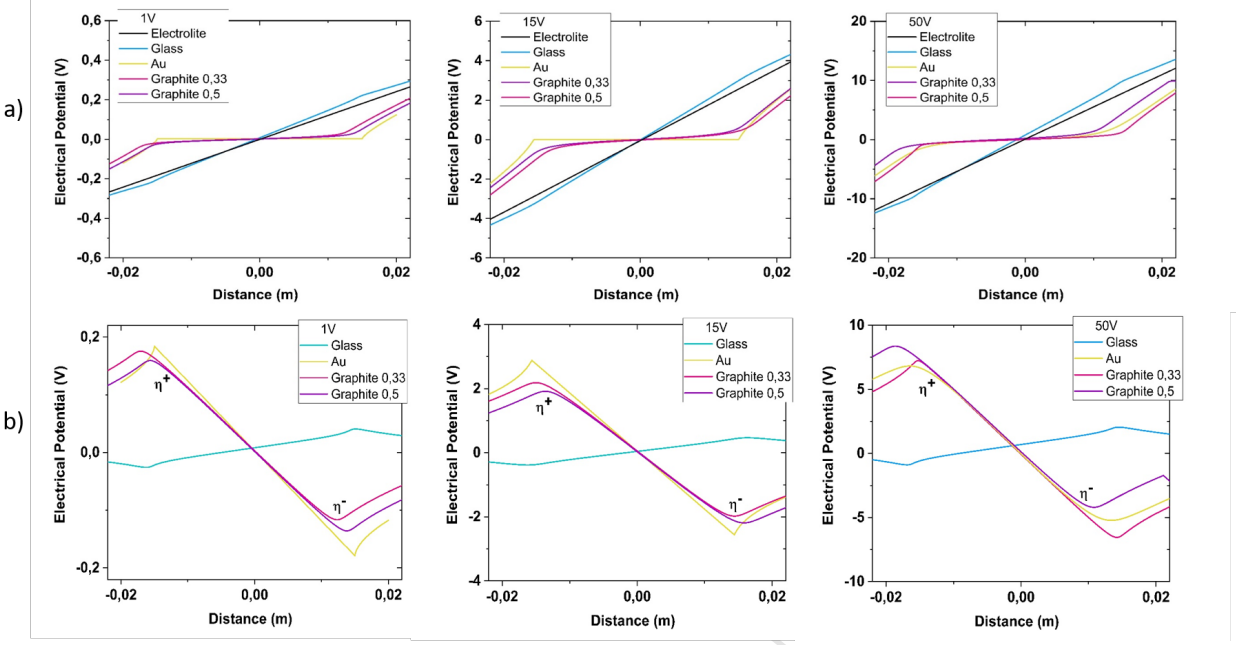

Figure 5

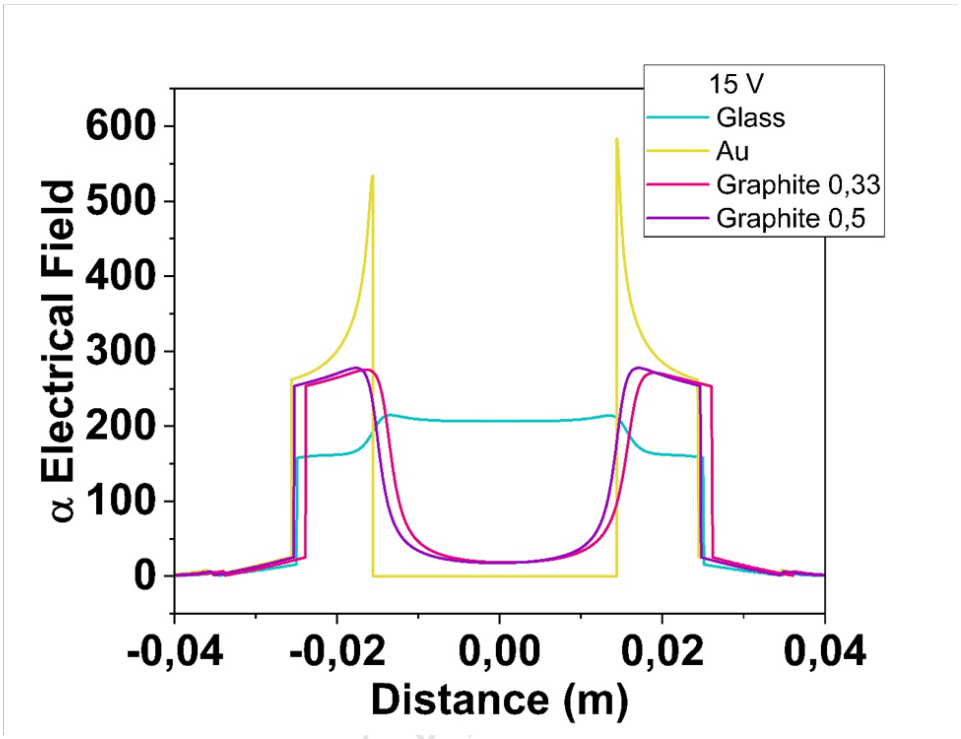

Figure 6

a)

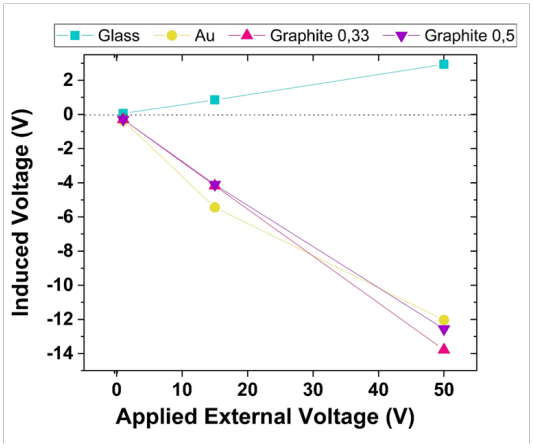

b)

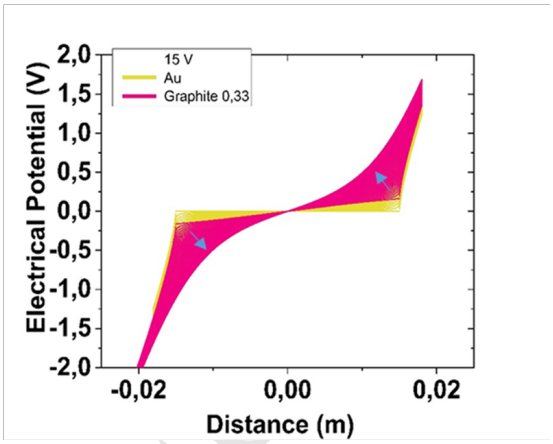

Research highlights

Finite element analysis shows inversion of voltage and charge gradient at immersed borders of conducting material as expected in bipolar electrochemistry effects

Intercalation materials show smaller and softer profiles of voltage and charge on the material surface than purely electronic conducting materials like gold

The dipolar effect extends to the whole material surface and reaches heights in the scale of neuron bodies, with about reduction of half of the voltage.

Finite element modelling envisages different charge and voltage gradients and spatial distribution for each material used previously in neuronal cell cultures, and may help explain the existence of various types of cell behavior.

Observations may explain the in vitro neural cell behavior in each material type, and may help to search for specific experimental gradients at specific locations.